

Retraction

Retracted: Medical Multimedia Image Analysis of Scoliosis in Children Aged 3–7 Years Based on Adaptive Multiobjective Differential Evolution Algorithm

Advances in Multimedia

Received 15 August 2023; Accepted 15 August 2023; Published 16 August 2023

Copyright © 2023 Advances in Multimedia. This is an open access article distributed under the Creative Commons Attribution License, which permits unrestricted use, distribution, and reproduction in any medium, provided the original work is properly cited.

This article has been retracted by Hindawi following an investigation undertaken by the publisher [1]. This investigation has uncovered evidence of one or more of the following indicators of systematic manipulation of the publication process:

- (1) Discrepancies in scope
- (2) Discrepancies in the description of the research reported
- (3) Discrepancies between the availability of data and the research described
- (4) Inappropriate citations
- (5) Incoherent, meaningless and/or irrelevant content included in the article
- (6) Peer-review manipulation

The presence of these indicators undermines our confidence in the integrity of the article's content and we cannot, therefore, vouch for its reliability. Please note that this notice is intended solely to alert readers that the content of this article is unreliable. We have not investigated whether authors were aware of or involved in the systematic manipulation of the publication process.

In addition, our investigation has also shown that one or more of the following human-subject reporting requirements has not been met in this article: ethical approval by an Institutional Review Board (IRB) committee or equivalent, patient/participant consent to participate, and/or agreement to publish patient/participant details (where relevant).

Wiley and Hindawi regrets that the usual quality checks did not identify these issues before publication and have since put additional measures in place to safeguard research integrity.

We wish to credit our own Research Integrity and Research Publishing teams and anonymous and named external researchers and research integrity experts for contributing to this investigation.

The corresponding author, as the representative of all authors, has been given the opportunity to register their agreement or disagreement to this retraction. We have kept a record of any response received.

References

- [1] C. Huang, "Medical Multimedia Image Analysis of Scoliosis in Children Aged 3–7 Years Based on Adaptive Multiobjective Differential Evolution Algorithm," *Advances in Multimedia*, vol. 2021, Article ID 9951035, 6 pages, 2021.

Research Article

Medical Multimedia Image Analysis of Scoliosis in Children Aged 3–7 Years Based on Adaptive Multiobjective Differential Evolution Algorithm

Chunxiang Huang 

Department of Physical Education, Wuyi University, Wuyishan 354300, Fujian, China

Correspondence should be addressed to Chunxiang Huang; wyshcx97@wuyiu.edu.cn

Received 21 July 2021; Accepted 20 August 2021; Published 30 September 2021

Academic Editor: Zhendong Mu

Copyright © 2021 Chunxiang Huang. This is an open access article distributed under the Creative Commons Attribution License, which permits unrestricted use, distribution, and reproduction in any medium, provided the original work is properly cited.

Scoliosis is mainly caused by the spinal column deviating from its centerline during the growth process. It usually occurs in children aged 3–7 years old. After a detailed analysis of the existing scoliosis detection methods, this paper compares and analyzes the advantages of using multimedia image processing technology to check scoliosis in children aged 3–7 years and uses an adaptive multiobjective differential evolution algorithm to perform scoliosis comprehensive testing. Finally, the experimental analysis shows that the adaptive multiobjective differential evolution algorithm is applied to scoliosis detection to analyze the characteristics of children's cervical spine curvature and the relationship between the cervical spine curvature and the scoliosis angle.

1. Introduction

The side of the spine is mainly the deviation of the spinal segment from the back center line with the coronal plane of the human body, resulting in the bending of the body to one side. Symptoms are spinal rotation and sagittal kyphosis and lordosis. There are many reasons for scoliosis [1–3]. Among them, the uncertain factor of the cause is also called idiopathic scoliosis. According to the survey of scoliosis, about 96.92% are idiopathic patients. Because the standards for measuring the lateral curvature of the spine are different, some scholars judge patients with a coronal face with a Cobb angle greater than 5° as scoliosis and patients with Cobb angles greater than 10° will be considered to have scoliosis. There are many ways to check for scoliosis. Generally, it can be divided into two kinds such as physical measurement methods and multimedia image analysis methods. The physical measurement method refers to the program that can directly touch the back of the human body when measuring scoliosis. It can be divided into Adams's anterior lens test, the use of scoliosis gauge to measure the rotation angle of the body, and the measurement of ribs.

The physical measurement method is based on people's work inspections. By investigating the spine side of a large

number of children between 3 and 7 years old, manual inspections are quite complicated and inefficient. In the detection of scoliosis, the multimedia image analysis method is a better method because in order to avoid manual participation, it improves efficiency and reduces the error caused by the doctor's subjective factors.

2. Adaptive Multiobjective Differential Evolution Algorithm

Adaptive multiobjective differential evolution consists of image parameter set, sequence parameter set, multimedia image parameter set, SEI in additional enhancement information, and image content information. All image data are compressed to the network adaptive unit. NALU includes two parts: header and load. In H.264/HEVC, the length of NALU header is fixed by two bytes, and the length of NALU load is an integer byte. H.264/HEVC also introduces access units, AU includes a plurality of NALUs arranged in the order of differential evolution, and these NALUs are differentially componentized to generate only one multimedia image. In some cases, ALU can be regarded as the basic unit of compressed bit stream. AU can start from

the boundary NALU, SEI-NALU, or NALU of the first SS. The length is fixed two bytes. The NALU payload length is an integer byte. VPS, SPS, PPS, and SEI are all separate NALUs, and Slice Segment CSS is also a separate NALU. However, the types are different. The former is non-VCL Video Coding Layer. The latter is VCL. In addition, H.264/HEVC also introduces access units. AU (access unit) includes multiple NALUs arranged in the order of differential evolution, and this NALU differential quantization only generates one multimedia image. In this case, the AU can be regarded as the basic unit of the compressed bit stream. The AU can start from the boundary NALU, SEI-NALU, or NALU of the first SS.

In the adaptive multiobjective differential evolution stage, each submultimedia image is treated as a slice/adaptive multiobjective differential evolution technology of H.265/HEVC [8–10]. As shown in Figure 1, each submultimedia image is treated as a slice/adaptive multiobjective differential evolution technology of H.265/HEVC. The target contains only one SS. Generally speaking, the SS adapting to multipurpose differential evolution has a VPSSPS and PPS. Before the adaptive multitarget difference of the submultimedia image is developed into a code stream, the header information of the submultimedia image needs to be updated accordingly. In order to initialize h correctly, the

differential evolver regenerates the corresponding initialization data. Different from the adaptive multitarget differential evolution composition, the adaptive multitarget composition is shown in Figure 2. All SSs in the target are AU and refer to PPS. Different AU reference PPS may also be different.

The whole evolution process of adaptive multiobjective differential is mainly divided into two modules. These two modules include the correction of code header information and the fusion of image content information. The modification of code stream header information mainly includes three-parts such as differential evolution, replacement, and coding of syntax elements.

First, the header information is differentially evolved to analyze the grammatical elements contained in the header information. Figure 3 shows the specific process.

The data bit stream segment of the multimedia image encoding output result can also be called SODB C String of Data Bits [11–13]. SODS is the highest storage form. After the SODS operation, load through initial raw byte sequence generates a compressed data containing SS, VSS, SPS, or PPS and other information generates a compressed data containing SS, VSS, SPS, or PPS and other information. Among them, the relationship between NALU, RBSP, and SODS is as follows:

$$\begin{aligned} \text{SODB} + \text{RBSP trailing bits} &= \text{RBSP}, \\ \text{NALU_header (2bits)} + \text{RBSP} &= \text{NALU}, \\ \text{Start Code Prefix} + \text{NALU} + \text{Start Code Prefix} + \text{NALU} + \dots &= \text{H.265 Bits Stream}. \end{aligned} \quad (1)$$

Therefore, to analyze the header information, it is necessary to first parse the code stream into multiple individual NALU, convert the NALU to RBSP, convert RBSP to SODS, and finally use the parsed SODS to obtain the relevant grammatical elements.

3. Materials and Methods

During the period from May 2011 to February 2017, 126 cases of scoliosis and bone disease were received and treated. Most of them were 3–7 years old, of which 84 were females and 42 were males. Among the 126 patients, there were 64 patients with congenital tumors in the spinal canal and syringomyelia, and 50 patients had a higher dose and a lower spinal cord. The thickness of the reconstructed data after importing the data from the Siemens workstation was 0.7 mm. After reconstructing them in three dimensions, 158 bone crests were extracted.

3.1. Method. Observe the morphology of the bone crest: take the transverse axis of the bone crest (pass through the center of the long axis of the bone in the sagittal plane and in the upper and lower edges of the vertebral body parallel to the coronal plane). Through the sagittal view of the bone crest and the transverse axis of the bone crest, carefully observe

the 158 bone crests, respectively. It will be observed that some of the bone crests have no bifurcation, and some of the bone crests appear to be bifurcated. Usually, the bone ridge without bifurcation is called the regular bone ridge, and the bifurcated bone ridge is called the irregular bone ridge, and they are carefully observed and counted separately.

Measure regular bone crests: measure the rear, middle, and front ends of each bone crest in the sagittal and transverse positions, respectively, in the sagittal position and the transverse axis, and use the diameter line as the basis to divide the bone ridge shapes into different types, Type I (thickness in the front, thin in the middle, and greater than the back in the front), Type II (thin in the front, thick in the middle, and smaller than the back in the front), Type III (thin in the middle, thick in the front and back, and the front is equal to the back), Type W (the middle is bigger than the back, the front is bigger than the middle), V type (front is equal to middle and equal to back), can type (front is less than back and less than middle), welcome type (front is less than middle and equal to back), which type (middle is equal to back and front is greater than Middle), and IX (front is less than back and equal to middle). The numbers of the above types were recorded in the sagittal position and the horizontal axis, respectively, according to the segment; the bone ridge morphology was observed in the coronal position.

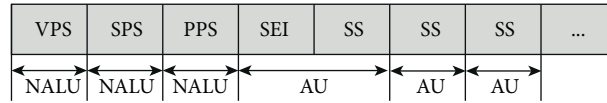


FIGURE 1: Adaptive multiobjective differential evolution method.

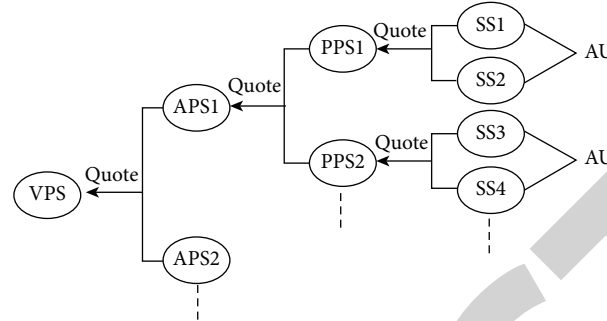


FIGURE 2: Complete self-adaptive multitarget composition method.



FIGURE 3: Process of parsing header information.

Observe irregular bone crests: observe irregular bone crests from different angles, which can be divided into three types: Type I (rear branch, front with base plate), Type II (front branch, rear with base plate), and Type III (middle part connection, front and rear Branch).

3.2. *Statistical Analysis.* Including data in SPSS19.0 software package, measurement data are expressed as $(x \pm s)$; data comparison between groups adopts t -test; count data are expressed in %; data comparison between groups adopts the chi-square test; and if $P < 0.05$, it means the difference is obvious.

4. Multimedia Image Analysis of Scoliosis Examination

Multimedia image analysis mainly focuses on scoliosis detection methods under two-dimensional images and three-dimensional images. The multimedia measurement methods used all use feature values related to spine symmetry. Usually, the multimedia images are acquired first, the images are processed, and the images are extracted to reflect the symmetry. The characteristic value of the degree of sexual damage ultimately determines the scoliosis of the child's body.

4.1. *X-Ray Film Measurement Method.* In the clinical use of scoliosis, X-ray images of the patient's back are usually taken, and the Cobb angle is marked on the X-ray images, and the actual degree of the Cobb angle is measured with a goniometer. This method is simple and correct, but it is judged by human

intervention. In addition, multimedia image processing technology can also be used to measure the Cobb angle of X-ray-based scoliosis images. However, X-rays are radioactive. It is not good for the growth of children from 3 to 7 years old.

4.2. *Method for Discriminating Based on the Features of Two-Dimensional Multimedia Images.* Curvature of the spine will cause the left and right sides of the back to be unequal, so the moiré multimedia image in the Moiré contour can play a role in small disturbances. We can use the moiré multimedia image to check the scoliosis of the spine. The measures and methods of using moiré multimedia image detection will be analyzed and explained.

For the examination of scoliosis of the spine, Kim et al. collected a large amount of data in the article and used a variety of judgment and explanation methods to carry out the examination. The main basis for checking the lateral curve of the spine is to see if the back features are equivalent, the center line of the back is used for detection in most articles. A detailed explanation of the axis of symmetry is the origin of the center line of the back.

As shown in Figure 4, $f(x, y)$ is used to represent the original moiré multimedia image and $f^{\text{ref}}(X, Y)$ is used to represent the multimedia image that $f(x, y)$ is symmetric about the $y = x \tan \theta$ axis. Choose to make

$$E = \sum_{(x,y) \in D} (f(x, y) - f^{\text{ref}}(X, Y))^2 \quad (2)$$

Ensure that it reaches the minimum θ and translation (u, v) , where D is the plane area where the multimedia image is located.

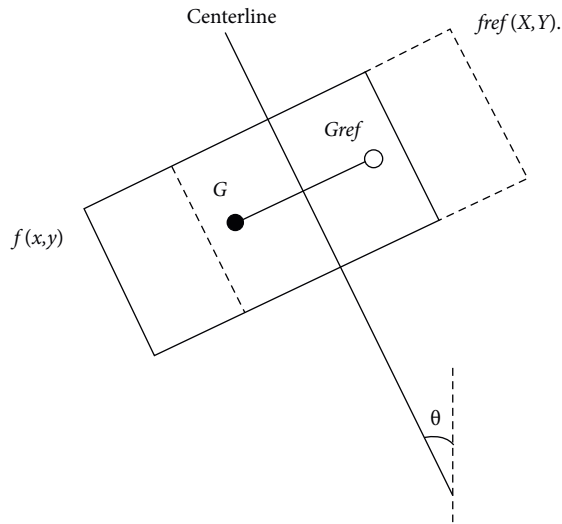


FIGURE 4: Schematic diagram of the method of extracting the center line from the back of the human body.

$$u + v \tan \theta = 0 \begin{pmatrix} X \\ Y \\ 1 \end{pmatrix} = \begin{pmatrix} \cos 2\theta & \sin 2\theta & u \\ \sin 2\theta & -\cos 2\theta & v \\ 0 & 0 & 1 \end{pmatrix} \begin{pmatrix} x \\ y \\ 1 \end{pmatrix}. \quad (3)$$

Then, use the gray-scale centroid calculation method to calculate the centroids G and $f^{\text{ref}}(X, Y)$ of $f(x, y)$ and $f^{\text{ref}}(X, Y)$, and then the vertical bisector connecting the two is the center line of the back of the human body.

Based on the centerline, Kim extracts different feature values for scoliosis and uses different inspection methods to detect patients. The detailed detection method and detection discrimination rate are shown in Table 1.

In addition to the identification of scoliosis under the above five characteristic values, the corresponding approach is shown in Figure 5. It can be seen that the center point P of the head, the center point Q of the waist, and PQ are the center lines of the human back. Then, the two points h and E can be extracted from the asymmetric Moiré fringe on the outermost side of the scapula, and the connecting line is perpendicular to PQ . In addition, the line GD is cut at the highest point of the same moiré, and PQ is transmitted to point A . The PQ cross waist intersects at point B of the moiré fringe, and the vertical line of PQ crosses over B to cross at points I and $F2$. Set $d1 = (CH + CE)/2$, $d2 = (AG + AD)/2$, and $d3 = (BF + BD)/2$, then $\tan \angle CAO = |d1 - d2|/CA$ and $\tan \angle CBO = |d1 - d3|/BC$, so the calculation formula of the Cobb angle is $\Theta = \angle CAO + \angle CBO$.

In the domestic research literature, many research scholars use the construction of the Cobb angle to diagnose the patient with projection moiré. According to the examination results, the patient's lumbar disc herniation can be obtained to explore the patient's waist relationship, and the patient can be treated according to the examination results. The cause of the tilt and rotation of the pelvis at the patient's position is detected. If it is detected that there is more than 1 ripple difference, the patient is judged as unqualified.

This test experiment shows that the results of patients measured by the moiré method are the same as those measured by X-rays.

4.3. Methods of Discrimination Based on Multimedia Image Features. In the detection process of scoliosis using the corresponding multimedia image of the back of the human body [14, 15], it is necessary to use multimedia imaging technology to perform three-dimensional reconstruction of the patient or use a laser scanner to scan the back to directly obtain the multimedia image.

After extracting the back features of the human body, the multimedia images of 111 patients were trained using the support vector machine principle, and the best coefficient set was derived to detect scoliosis. Comparing the discriminant results using support vector machines, decision trees, and linear discriminants, the discriminant rates obtained were 85%, 77%, and 78%, respectively.

Using the ISIS (Integrated Shape Imaging System), they developed to find the height of the human body. Figure 6 shows the working principle of the ISIS. The parallel rectangle is projected onto the back of the human body to extract the moiré multimedia image data of the back. The Fourier transform contour technique is used to reconstruct the three-dimensional negligence of the back to extract the data $h(x, y) = l_0 \varphi_H(x, y) / \varphi_H(x, y) - 2\pi f_0 d_0$ of the back of the human body. In the formula, l_0 represents the distance between the entrance pupil of the camera and the selected reference plane, $\varphi_H(x, y)$ represents the phase corresponding to the measured target H point, f_0 represents the grating frequency, and d_0 represents the distance between the entrance pupil of the camera and the exit pupil of the projector.

Before using the multimedia image analysis method to obtain the patient's medical images, you need to mark the position of the spine on the spine, and then according to the approximate position of the spine, L is the vertical line; according to a, as shown in Figure 7, the position of this part mainly uses the doctor's touch to get the patient's back. After the three-dimensional reconstruction, the accurate position of the spine is measured according to the skin angle, and the vertical line passing through the carina is used as the centerline of the human back according to medical knowledge, and the back features are extracted: (1) the sacral bone d to the vertical vertebra passing through the carina, the distance of the line L . (2) The difference in volume between the left and right sides of the back. The dotted line in Figure 6 is the measured spine.

Through the experimental comparison of 168 patients, the angle θ measured by SIS2 is compared with the Cobb angle measured by X-rays, and it has a correlation of $r = 0.84$.

According to the above discussion, the curvature of the spine is detected by reorganized multimedia images. Under normal circumstances, when the position of the spine is known, the feature is obtained by the joint position of the spine to detect the curvature of the spine. If the 3D reconstruction data are accurate using a laser scanner such as Ramirez, the inspection cost of this method is high and it is not popularized. Compared with the above two methods,

TABLE 1: Comparison of the detection of scoliosis in different papers such as the study by Kim.

Literature number	Extracted features	Value detection method	Total number of cases	Recognition rate (%)
10	μ, σ	Linear discriminant	120	88.4
11	μ, σ	BP neural networks	1200	89.1
12	$\mu, \sigma,$	BP neural networks	1200	90.4
13	$\mu, \sigma, \mu_d, \sigma_d$	Support vector machines	1200	85.4
14	μ, σ, C	CBP neural networks	1200	85.5

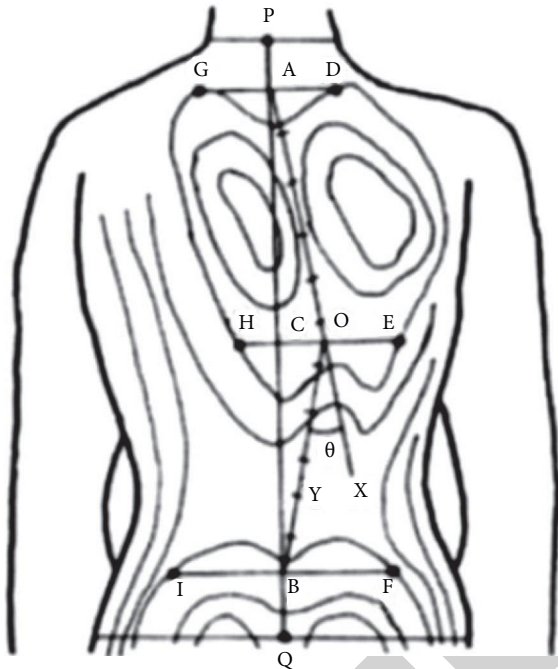


FIGURE 5: Schematic diagram of obtaining the Cobb angle.

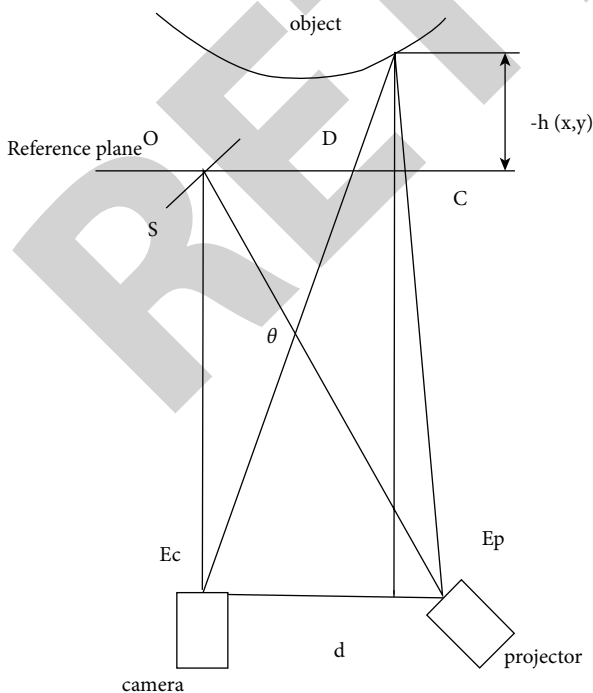


FIGURE 6: Schematic diagram of ISIS measurement principle.

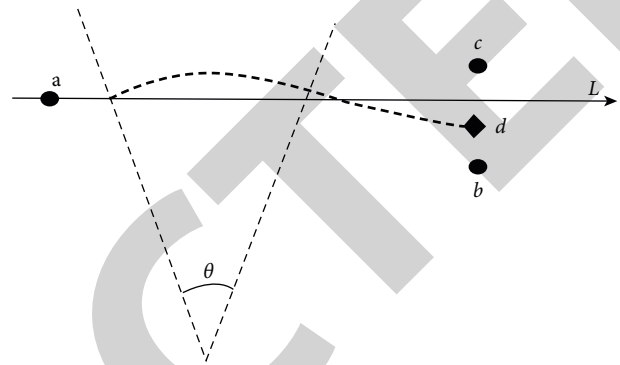


FIGURE 7: Schematic diagram of back 3D feature extraction.

Berryman et al. can achieve good reconstruction accuracy in the form of structured light, and at the same time, the cost is reasonable.

5. Conclusions

This article is using multimedia image processing technology for the examination of scoliosis in children aged 3–7 and the adaptive multiobjective differential evolution algorithm to obtain the three-dimensional features of scoliosis. After evaluating the advantages and disadvantages of the current multimedia image processing methods, the results are obtained. Compared with the evaluation model, the method in this paper can find the position of scoliosis more accurately and is suitable for the inspection of any part of the back of the body. Therefore, the adaptive multiobjective difference method is more accurate than the traditional algorithm, and it also appears to have more research value.

Data Availability

The data used to support the findings of this study are available from the corresponding author upon request.

Conflicts of Interest

The author declares that there are no conflicts of interest.

References

- [1] A. Blomkvist, K. Olsson, and M. N. Eek, “The effect of spinal bracing on sitting function in children with neuromuscular scoliosis,” *Prosthetics and Orthotics International*, vol. 42, no. 6, pp. 592–598, 2018.
- [2] V. Sataev, P. Mironov, D. Yunusov, A. Farkhshatov, and T. Psyanchin, “Scoliosis: surgical treatment in children,”

- Medical News of North Caucasus*, vol. 11, no. 2, pp. 39–45, 2016.
- [3] M. Puttagunta and S. Ravi, “Medical image analysis based on deep learning approach,” *Multimedia Tools and Applications*, vol. 80, no. 13, pp. 1–34, 2021.
- [4] Y. Zheng, X. Wu, Y. Dang, Y. Yang, J. D. Reinhardt, and Y. Dang, “Prevalence and determinants of idiopathic scoliosis in primary school children in Beitang district, Wuxi, China,” *Journal of Rehabilitation Medicine*, vol. 48, no. 6, pp. 547–553, 2016.
- [5] S. Moalej, S. Kazemi, M. Asadabadi et al., G. Shariatpanahi, “Screening of scoliosis in school children in Tehran: the prevalence rate of idiopathic scoliosis,” *Journal of Back and Musculoskeletal Rehabilitation*, vol. 31, pp. 1–8, 2018.
- [6] R. Wang, J. Lv, and S. Ma, “A MRI image segmentation method based on medical semaphore calculating in medical multimedia big data environment,” *Multimedia Tools and Applications*, vol. 24, no. 1, pp. 181–186, 2017.
- [7] F. Hengwei, H. Zifang, W. Qifei et al., “Prevalence of idiopathic scoliosis in Chinese schoolchildren,” *Spine*, vol. 41, no. 3, pp. 259–264, 2016.
- [8] Z. He, Y. Wang, X. Qin et al., “Classification of neurofibromatosis-related dystrophic or nondystrophic scoliosis based on image features using bilateral CNN,” *Medical Physics*, vol. 48, pp. 1571–1583, 2021.
- [9] M. R. Konieczny, J. Boos, A. Steuwe, C. Schleich, M. Prost, and R. Krauspe, “Effective dose of radiation per screw in surgery of adolescent idiopathic scoliosis: matched pair analysis of 293 pedicle screws inserted using three different techniques,” *Journal of Children’s Orthopaedics*, vol. 14, no. 6, pp. 554–561, 2020.
- [10] D. Truumees, A. Duncan, E. K. Mayer, M. Geck, D. Singh, and E. Truumees, “Cross sectional analysis of scoliosis-specific information on the internet: potential for patient confusion and misinformation,” *Spine Deformity*, vol. 8, no. 6, pp. 1159–1167, 2020.
- [11] B. Ionescu, H. Müller, R. Péteri, D. T. Dang-Nguyen, and M. G. Constantin, “Imageclef 2020: multimedia retrieval in lifelogging,” *Medical, Nature, and Internet Applications*, vol. 8, no. 1, pp. 46–58, 2020.
- [12] S. Al-Zu’bi, B. Hawashin, A. Mughaid, and T. Baker, “Efficient 3d medical image segmentation algorithm over a secured multimedia network,” *Multimedia Tools and Applications*, vol. 80, no. 3, pp. 1–19, 2020.
- [13] A. I. Tsirikos, S. B. Roberts, and E. Bhatti, “Incidence of spinal deformity surgery in a national health service from 2005 to 2018: an analysis of 2,205 children and adolescents,” *Bone and Joint Open*, vol. 1, no. 3, pp. 19–28, 2020.
- [14] N. K. Pareek and V. Patidar, “Medical image protection using genetic algorithm operations,” *Soft Computing*, vol. 20, no. 2, pp. 763–772, 2016.
- [15] J. R. Panchmatia, A. Isaac, T. Muthukumar, A. J. Gibson, and J. Lehovsky, “The 10 key steps for radiographic analysis of adolescent idiopathic scoliosis,” *Clinical Radiology*, vol. 70, no. 3, pp. 235–242, 2015.